

# Merg1a K<sup>+</sup> channel induces skeletal muscle atrophy by activating the ubiquitin proteasome pathway

Xun Wang,\* Gregory H. Hockerman,<sup>†</sup> Henry W. Green III,<sup>‡</sup> Charles F. Babbs,\* Sulma I. Mohammad,<sup>§</sup> David Gerrard,<sup>¶</sup> Mickey A. Latour,<sup>¶</sup> Barry London,<sup>||</sup> Kevin M. Hannon,\*<sup>1</sup> and Amber L. Pond\*,<sup>1,2</sup>

\*Department of Basic Medical Sciences, School of Veterinary Medicine; <sup>†</sup>Department of Medicinal Chemistry and Molecular Pharmacology, College of Pharmacy; <sup>‡</sup>Department of Veterinary Clinical Sciences, School of Veterinary Medicine; <sup>§</sup>Department of Veterinary Pathobiology and Cancer Center; and <sup>¶</sup>Department of Animal Sciences, College of Agriculture, Purdue University, West Lafayette, Indiana, USA; and <sup>||</sup>Cardiovascular Institute, University of Pittsburgh, Pittsburgh, Pennsylvania, USA

**ABSTRACT** Skeletal muscle atrophy results from an imbalance in protein degradation and protein synthesis and occurs in response to injury, various disease states, disuse, and normal aging. Current treatments for this debilitating condition are inadequate. More information about mechanisms involved in the onset and progression of muscle atrophy is necessary for development of more effective therapies. Here we show that expression of the mouse ether-a-go-go related gene (Merg1a) K<sup>+</sup> channel is up-regulated in skeletal muscle of mice experiencing atrophy as a result of both malignant tumor expression and disuse. Further, ectopic expression of Merg1a in vivo induces atrophy in healthy wt-bearing mice, while expression of a dysfunctional Merg1a mutant suppresses atrophy in hindlimb-suspended mice. Treatment of hindlimb-suspended mice with astemizole, a known Merg1a channel blocker, inhibits atrophy in these animals. Importantly, in vivo expression of Merg1a in mouse skeletal muscle activates the ubiquitin proteasome pathway that is responsible for the majority of protein degradation that causes muscle atrophy, yet expression of a dysfunctional Merg1a mutant decreases levels of ubiquitin-proteasome proteolysis. Thus, expression of Merg1a likely initiates atrophy by activating ubiquitin-proteasome proteolysis. This gene and its product are potential targets for prevention and treatment of muscle atrophy.—Wang, X., Hockerman, G. H., Green, H. W. III, Babbs, C. F., Mohammad, S. I., Gerrard, D., Latour, M. A., London, B., Hannon, K. M., Pond, A. L. Merg1a K<sup>+</sup> channel induces skeletal muscle atrophy by activating the ubiquitin proteasome pathway. *FASEB J.* 20, E803–E811 (2006)

**Key Words:** *ectopic gene expression • hindlimb suspension • astemizole*

SKELETAL MUSCLE ATROPHY, a reduction of contractile protein content and muscle strength, can result from muscle damage, disease, disuse or aging (1–4); the resultant debilitation can seriously compromise quality

of life. Physical therapy and administration of growth factors (5), inhibitors of proteolysis (6), or stimulators of protein synthesis (7) are methods being studied to treat atrophy; however, more effective treatments are needed. The ubiquitin proteasome pathway (UPP), by which protein substrates are degraded (8), is prominent among mechanisms known to modulate skeletal muscle atrophy; however, little is known about the factors activating this pathway.

The erg1 (Kv11.1, KCNH2) K<sup>+</sup> channel conducts I<sub>Kr</sub> current, which is partially responsible for repolarization of the cardiac action potential in many mammalian species, including mice and humans. Mutations in human erg1 (HERG1) can produce Long QT Syndrome (LQT2), an inherited cardiac disorder characterized by delay of cardiac repolarization, syncope, ventricular arrhythmias, and risk of sudden death (9). Erg1 K<sup>+</sup> channels are composed of four separate  $\alpha$ -subunit proteins. Two alternative splice variants of the erg1  $\alpha$ -subunit have been cloned from mouse (Merg1a and 1b; 10) and human (HERG1A and 1B; 11) cDNA libraries. The Merg1b alternative splice variant lacks the first 380 amino acids found in the 1a subunit and, instead, begins with 40 unique amino acids (10). Electrophysiological studies show that distinct functional K<sup>+</sup> channels are produced by expression of each splice variant alone and by coexpression of both (10, 11). A recent report indicates that in vivo cardiac I<sub>Kr</sub> current is produced by a heteromultimeric erg1 channel, composed of two 1a and two 1b subunits (12). High levels of erg1a protein have been detected in adult heart and brain tissues of various mammals (10–14). Merg1 gene expression is detected in numerous tissues of embryonic mice, including skeletal muscle (13). To our knowledge, there are no reports of erg1a gene

<sup>1</sup> These authors contributed equally to this work.

<sup>2</sup> Correspondence: School of Veterinary Medicine, Purdue University, 625 Harrison St., West Lafayette, IN 47907, USA. E-mail: pond@purdue.edu  
doi: 10.1096/fj.05-5350fe

expression in adult mammalian skeletal muscle or of a role for *erg1* function in modulation of proteolysis. Here we show that *erg1*, a voltage-gated  $K^+$  channel, is up-regulated in atrophic skeletal muscle of mice. Further, ectopic expression of Merg1a in skeletal muscle induces UPP proteolysis and atrophy, while ectopic expression of a dysfunctional dominant negative Merg1a (DN Merg1a, G628S; 15) mutant decreases UPP proteolysis and inhibits atrophy in hindlimb-suspended mice. The data suggest that Merg1a participates in the onset of skeletal muscle atrophy by signaling increased UPP proteolysis.

## MATERIALS AND METHODS

**Animals** All procedures were approved by the Purdue Animal Care and Use Committee. ND4-Swiss Webster mice (Harlan-Sprague, Indianapolis, IN) were used in all procedures except for tumor studies which used athymic mice (NCR-nu; Harlan-Sprague). Animals were housed in Purdue University facilities, monitored by lab animal veterinarians and provided food and water ad libitum.

### Hindlimb suspension

Custom suspension cages were constructed as described previously (16). Mice were placed in these cages resting in approximately a 30° head down tilt with their hindlimbs elevated so that they were unable to place any load on their hindlimbs. Control mice were kept in commercial mouse cages in a normal wt-bearing state.

### Tumor induction

Kb human esophageal cancer cells (7000 cells/100  $\mu$ l of RPMI medium with 10% FBS and 1% glutamine; 17) were implanted subcutaneously (s.c.) in the right axilla of athymic mice ( $n=8$ ; NCR-nu; Harlan-Sprague). Control mice ( $n=8$ ) were injected with vehicle. Mice were weighed weekly for 6 wk. Tumors were measured by a digital caliper biweekly.

### Western blot

For immunoblots, membrane proteins were extracted from gastrocnemius muscles and brain (14). Samples were immunoblotted by using *erg1* antibody (Ab) (14). After blotting, membranes were stained with 0.1% Coomassie R-250 to confirm that membrane samples contained equal protein.

### Tissue sections and staining

Gastrocnemius muscles were prepared and cryo-sectioned (14  $\mu$ m) as described earlier (16). Sections were stained for  $\beta$ -galactosidase (lacZ) activity (16) or immunostained (16) using *erg1* Ab (14), except where noted. Images of sections were captured with a Leaf Micro-Lumina digital camera (Scitex; Tel-Aviv, Israel). The pixel number of each muscle fiber cross section was determined (Adobe Photoshop 6) and converted to  $\mu$ m<sup>2</sup>. Two sections (50 fibers each) from each muscle mid-section were analyzed.

## Plasmids

The Merg1a (10), Merg1b (10) and DN-Merg1a (G628S; 15) clones were in pBK/cytomegalovirus (CMV). The ubiquitinated firefly luciferase (Ub-FL) in pGL-3/CMV was a gift from Dr. David Piwnicka-Worms (18; Washington University, St. Louis, MO). The CMV-nlacZ in pNL vector was purchased from the Center Commercial de Gros (Toulouse, France). The phRL synthetic *Renilla* luciferase (RL) reporter vector was purchased from ProMega (Madison, WI).

## Electroporation

Mice were anesthetized with 0.01  $\mu$ l/mg body wt of xylazine (1 mg/ml) and ketamine (9 mg/ml) in sterile saline. Gastrocnemius muscles of shaved hindlimbs were injected with plasmids and electroporated with 8 pulses at 200V/cm for 20 ms at 1 Hertz (19) with an extracellular matrix (ECM) 830 ElectroSquare Porator (BTX; Hawthorne, NY).

## Reverse-transcription polymerase chain reaction (RT-PCR)

RT-PCR was performed as described earlier (16), except that contaminating DNA was removed from total RNA extract by two 10-min treatments with DNase I (ProMega). Duplicate RNA samples were exposed either to reverse-transcriptase or to vehicle only. Template control samples did not receive RNA. The reverse-transcription product was amplified with PCR, combined with ethidium bromide, and electrophoresed on a 2% agarose gel. Primers for Merg1a were: 5' – CGC AGA ACA CCT TCC TCG ACA C – 3' (forward) and 5' – GCA GAA GCC GTC GTT GCA GTA G – 3' (reverse). Primers for Merg1b were: 5' – AGT CCT CCA TGG CGA TTC – 3' (forward) and 5' – GGC CTG CAG CTT ATA CTC – 3' (reverse).

*Astemizole* (Sigma, St. Louis, MO)

The antihistamine astemizole (20) was suspended in water.

## ECG

Mice were anesthetized by a 240 mg/kg body wt i.p. injection of 20 mg/ml Avertin (2, 2, 2-tribromoethanol; Sigma) in a solution of 1.25% tert-amyl alcohol in saline (21). A standard lead II ECG was obtained by placing 18-gauge needle electrodes s.c. in the right foreleg (–), left hind leg (+), and right hind leg (ground). ECG's were recorded (3 min) using a multichannel Biopac MP100 physiological recording system (Biopac Systems Inc; Goleta). QT intervals were measured and corrected for heart rate using the formula:  $QT_C = QT_O / (RR_O / 100)^{0.5}$  (22).

## Dual luciferase reporter assay

The Dual-Luciferase Reporter Assay Kit (Promega) was used in accordance with manufacturer's instructions. Firefly luciferase and *Renilla* luciferase (RL) activities were measured with a TD-20/20 Luminometer (Promega).

## Statistics

Data were analyzed by ANOVA for a completely randomized design. When significant differences were found, means were separated by Fisher's Protected Least-Significance Difference. All data were analyzed using the General Linear Model Procedure of SAS. Statements of significance were based on *P*-levels as noted.

## RESULTS

### Tumor expression induces Merg1a synthesis and atrophy in skeletal muscle

Six weeks after injection of tumor cells, the average wt of tumor-bearing mice (minus tumor wt) was 10.8% ( $P \leq 0.005$ ) less than control mice. Tumor-expressing mice had an 18% ( $P \leq 0.001$ ) lower gastrocnemius wt-to-body wt ratio ( $1.10 \pm 0.019\%$ , SEM) than control mice ( $1.34 \pm 0.018\%$ , SEM), demonstrating that tumor bearing mice lost muscle mass. The mean muscle fiber cross-sectional area (csa) of left gastrocnemius muscles from tumor-bearing mice was 25% less ( $P \leq 0.05$ ) than that of control mice ( $1445.8 \pm 103.8 \mu\text{m}^2$  SEM vs.  $1925.0 \pm 161.6 \mu\text{m}^2$  SEM, respectively), demonstrating that tumor-bearing mice experienced skeletal muscle atrophy. Western blot analysis of extracted membrane proteins detected two Merg1a proteins in cachectic mouse skeletal muscle as previously reported in brain and heart (14; **Fig. 1A**). No Merg1 channel protein was detected in control tissue (**Fig. 1A**).

### Hindlimb suspension results in atrophy and Merg1a synthesis in skeletal muscle

Fourteen mice were hindlimb-suspended (16) for either 4 ( $n=7$ ) or 7 ( $n=7$ ) d, while control animals ( $n=14$ ) remained wt bearing. Left gastrocnemius muscles were embedded and cross sectioned, while right muscles were analyzed with Western blot (14) and RT-PCR analyses (16). After 7 d, relative to control animals, suspended mice experienced a mean 25% decrease ( $P \leq 0.005$ ) in ratio of gastrocnemius muscle wt to body wt and a 45% decrease ( $P \leq 0.05$ ) in muscle fiber csa. Data show that hindlimb suspension induced atrophy in gastrocnemius muscles. Western blot analysis (14) detected two Merg1a protein isoforms in atrophying skeletal muscle, but not in controls (**Fig. 1B**). Consistently, Merg1a mRNA was detected in atrophic muscle (**Fig. 1C**). A substantially lower concentration of Merg1a message was also detected in control muscle (**Fig. 1C**, lane 3), suggesting that Merg1a protein is synthesized in this tissue at levels not detectable by our Western blotting procedure. After concentrating (4 $\times$ ) a control gastrocnemius muscle sample, Merg1a proteins were evident by blotting (**Fig. 1D**). We did not detect proteins in the skeletal muscle sample that correlated to the predicted mass of Merg1b protein (95 kDa; **Fig. 1D**). Indeed, RT-PCR analysis failed to detect Merg1b message in either control or atrophied muscle (**Fig. 1E**). Using immunohistochemistry (16), we demonstrated that Merg1 proteins were localized in atrophic skeletal muscle fibers; none was found in control muscle (**Fig. 1F**).

### Electroporation results in expression of plasmid DNA

Left gastrocnemius muscles of 14 mice were injected with expression plasmid encoding Merg1a (30  $\mu\text{g}$ ; 10),

while left gastrocnemius muscles of another 14 mice received expression plasmid encoding Merg1b (30  $\mu\text{g}$ ; 10). Right gastrocnemius muscles of all mice were injected with expression plasmid encoding lacZ (30  $\mu\text{g}$ ; 10). Gastrocnemius muscles were electroporated to facilitate plasmid uptake (19). After 7 d, Merg1a proteins (14) were detected in Merg1a injected muscles by Western blot analysis; these proteins were not detected in control muscle (**Fig. 2A**). A Merg1b protein was detected just above 95 kDa in muscles injected with Merg1b plasmid; this protein was absent from control muscle (**Fig. 2B**).

### Merg1a expression in wt-bearing mice induces skeletal muscle atrophy

Left gastrocnemius muscles of 14 mice were injected with lacZ (20  $\mu\text{g}$ ) and control (40  $\mu\text{g}$ ) expression plasmids. Right gastrocnemius muscles of seven of these mice were coinjected with Merg1a (20  $\mu\text{g}$ ; 10), lacZ (20  $\mu\text{g}$ ) and control pBK/CMV DNA expression plasmids (20  $\mu\text{g}$ ). The right gastrocnemius muscles of the remaining mice ( $n=7$ ) were coinjected with three expression plasmids, each encoding for either: Merg1a (20  $\mu\text{g}$ ; 10), lacZ (20  $\mu\text{g}$ ), or a dominant-negative Merg1a mutant (DN Merg1a; 20  $\mu\text{g}$ ; 15). The DN Merg1a gene product is a pore mutant that is transported to the cell membrane but prevents Merg1 current conduction (15). Mice remained wt-bearing. Seven days after electroporation, gastrocnemius fibers expressing Merg1a and lacZ (blue fibers) experienced a significant 16.3% decrease in muscle fiber csa relative to fibers injected with lacZ plasmid only (**Fig. 3A1, 2; B1, 2**). Blockade of Merg1a function by DN Merg1a prevented all but 6.7% of the atrophy induced by Merg1a expression (**Fig. 3A1, 3; B1, 3**). This incomplete rescue is not surprising, because it is not likely that all randomly assembled channels would contain mutant channel subunit.

### Block of Merg1a function inhibits the skeletal muscle atrophy induced by hindlimb suspension

Left gastrocnemius muscles of 14 mice were injected with lacZ expression plasmid (20  $\mu\text{g}$ ) and control plasmid (30  $\mu\text{g}$ ). Right gastrocnemius muscles received lacZ expression plasmid (20  $\mu\text{g}$ ) plus expression plasmid encoding DN Merg1a (30  $\mu\text{g}$ ; 16). Twelve hours after electroporation (19), mice were either hindlimb-suspended ( $n=7$ ) or remained wt-bearing ( $n=7$ ). After 7 d, there was a 45% decrease in csa of suspended mouse muscle fibers relative to wt-bearing controls, showing that suspension induced atrophy (**Fig. 3C1, 2; D1, 2**). Importantly, the muscle fibers from suspended mice expressing lacZ and DN Merg1a mutants (15) were 13.4% smaller than fibers from muscles of wt bearing mice expressing lacZ (**Fig. 3C2, 3; D**). Data demonstrate that, although DN Merg1a expressing fibers do not completely retain control fiber size (as expected), block of Merg1a function



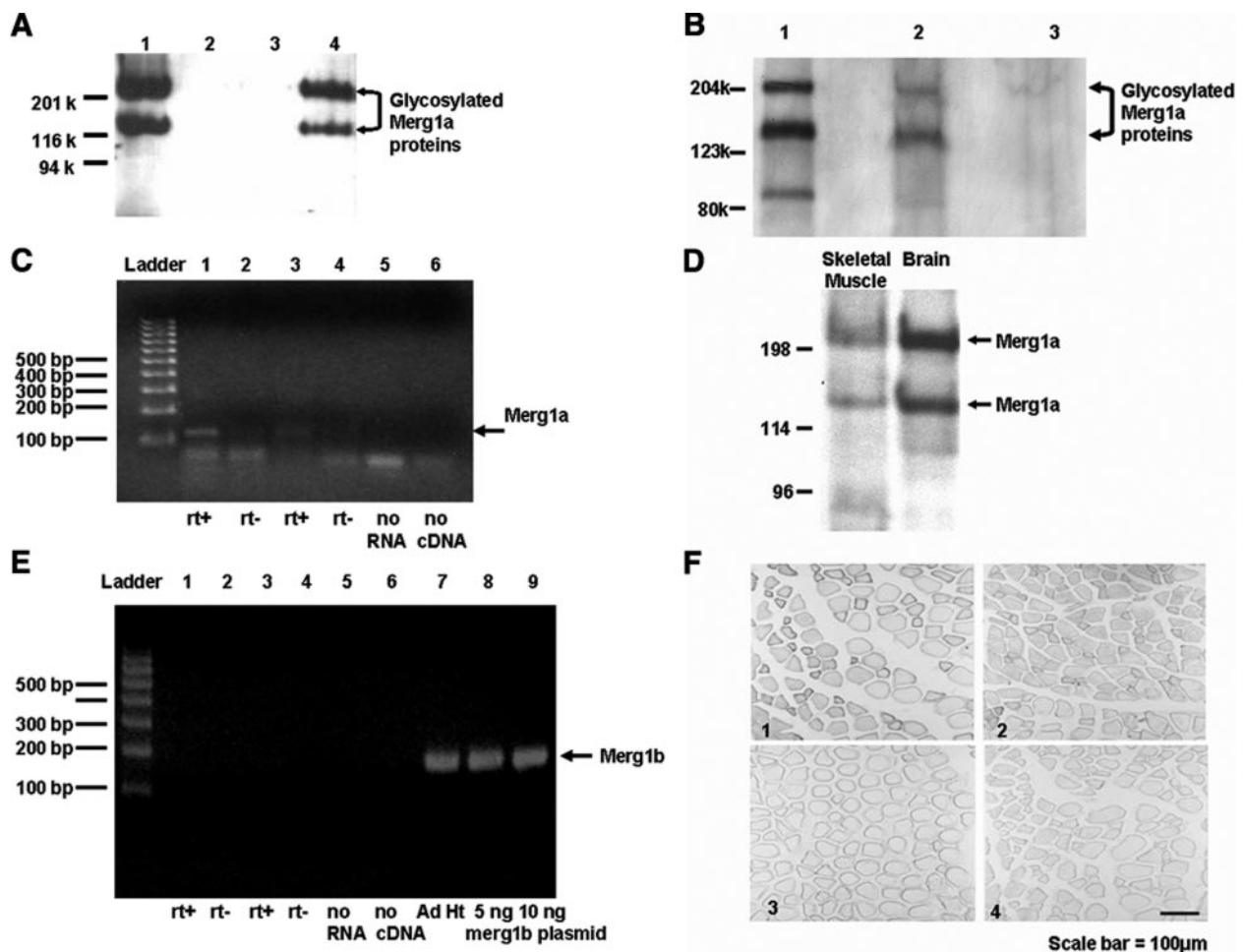


**Figure 1.** Merg1a  $K^+$  channel is expressed in atrophic gastrocnemius muscles of cachectic and hindlimb-suspended mice. *A*) Merg1a channel protein isoforms are detected in gastrocnemius muscles of mice experiencing atrophy as a result of malignant tumor growth. Western blot of membrane proteins from brain (positive control; lane 1, 15  $\mu$ g), control mouse gastrocnemius muscle (pooled muscles of 8 mice; lanes 2 and 3, 50 and 44  $\mu$ g, respectively), tumor-expressing mouse gastrocnemius muscle (pooled muscles of 8 mice; lane 4, 44  $\mu$ g). These qualitative results are representative of two animal trials. *B*) Merg1a proteins are detected in gastrocnemius muscles of hindlimb suspended mice. Western blot of membrane proteins from brain (positive control; lane 1, 15  $\mu$ g), skeletal muscle from suspended mice (pooled muscles of 10 mice; lane 2, 60  $\mu$ g) and skeletal muscle from wt-bearing mice (pooled muscles of 10 mice; lane 3, 60  $\mu$ g). These results are representative of three hindlimb-suspension trials. *C*) Merg1a mRNA is abundant in atrophic gastrocnemius muscle from hindlimb-suspended mice. RT-PCR shows that Merg1a mRNA is abundant in reverse-transcriptase-treated (rt+) total RNA sample extracted from skeletal muscle of mice suspended for 7 d (lane 1, 5 pooled muscles). Merg1a message is much less abundant in rt+ samples of total RNA extracted from skeletal muscle of wt-bearing mice (lane 3, 5 pooled muscles). Merg1a message was not detected in samples not treated with rt (rt-, lanes 2 and 4). Merg1a message was not detected in samples void of RNA (lane 5) or cDNA (lane 6), showing that the rt product detected is Merg1a. These results are representative of three separate hindlimb-suspension trials of 16 mice each. *D*) Low levels of Merg1a protein are detected in skeletal muscle of wt-bearing mice. Western blot of membrane proteins from concentrated (4 $\times$ ) control mouse gastrocnemius muscle sample (lane 1, 70  $\mu$ g) and from brain sample (positive control; lane 2, 15  $\mu$ g). The blot is representative of three samples composed of 10 pooled gastrocnemius muscles each. *E*) Merg1b mRNA is not detected in atrophic or control skeletal muscle. RT-PCR results demonstrate that Merg1b mRNA is not detected in reverse-transcriptase-treated (rt+) total RNA sample extracted from skeletal muscle of mice suspended for 7 d (lane 1) or muscle from wt-bearing mice (lane 3). Merg1b message was not detected in samples not treated with RT (rt-, lanes 2 and 4). Merg1b message was not detected in samples void of RNA (lane 5) or cDNA (lane 6), showing that RT product detected is Merg1b. Adult mouse heart (lane 7) and merg1b plasmid (lanes 8 and 9) were analyzed as positive controls. These results are representative of two animal suspension studies. *F*) Merg1a  $K^+$  channel protein is located in sarcolemmal membranes of skeletal muscle from hindlimb-suspended mice. Representative muscle sections from animals suspended for 4 (panel 1) and 7 (panel 2) d and immunostained with erg1 Ab. Representative muscle section (immunostained with erg1 Ab) from a wt-bearing animal (panel 3). Representative skeletal muscle section from suspended (4 d) mice immunostained without erg1 Ab (panel 4) as control. Scale bar = 100 $\mu$ m.

does attenuate atrophy. Further, DN Merg1a (15) and lacZ expressing fibers did not undergo atrophy to the extent of fibers from the same section not expressing plasmid DNA (Fig. 3D, compare stained

and nonstained fibers). Thus, synthesis of DN Merg1a mutant blocks the onset of disuse atrophy in suspended mice, showing that Merg1a current conduction plays a role in atrophy. Note: Expression of lacZ

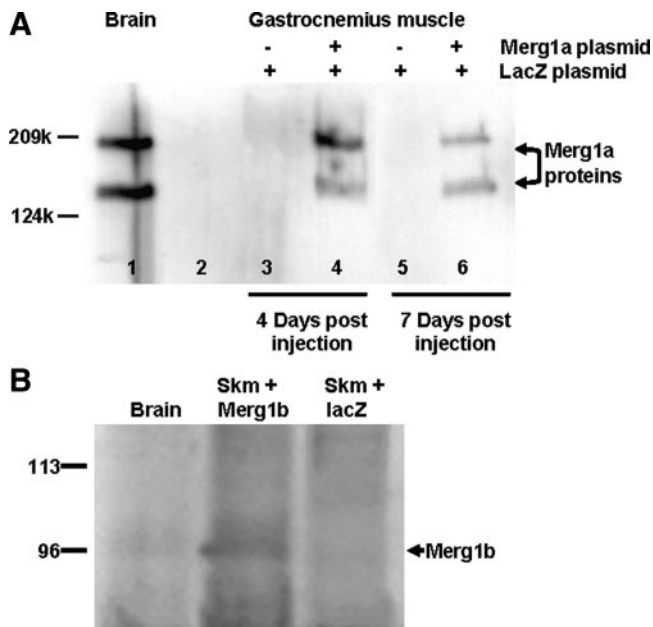


**Figure 2.** Injection of plasmid DNA followed by electroporation induces ectopic expression of encoded genes. *A*) Injection of Merg1a encoding plasmid into mouse gastrocnemius followed by electroporation results in synthesis of Merg1a protein. Western blot of membrane protein samples from: mouse brain (lane 1, 15  $\mu$ g), mouse gastrocnemius muscles (50  $\mu$ g) from wt-bearing mice injected with lacZ only (lane 3 is 4 d post-injection; lane 5 is 7 d post-injection), and from mice injected with lacZ and Merg1a (lane 4 is 4 d post-injection; lane 6 is 7 d post-injection). Lane 2 received buffer only. This figure is representative of three different electroporation trials. *B*) Injection of Merg1b encoding plasmid into mouse gastrocnemius followed by electroporation results in synthesis of Merg1b protein. Western blot of membrane proteins (15  $\mu$ g) from mouse brain membrane protein extract. Membrane proteins extracted from gastrocnemius muscles (pooled muscle of 10 mice; 50  $\mu$ g) of wt-bearing mice injected with lacZ and Merg1b or with lacZ only. This figure is representative of three different electroporation trials.

alone did not affect muscle fiber size in either wt-bearing or suspended mice (Fig. 3D 1, 2; compare stained and nonstained fibers within each section). This observation was confirmed by fiber csa (data not shown).

### Ectopic expression of Merg1b in gastrocnemius muscle does not induce atrophy

Left gastrocnemius muscles of seven mice were injected with lacZ expression plasmid (20  $\mu$ g) and control expression plasmid (30  $\mu$ g), while right gastrocnemius muscles received lacZ expression plasmid (20  $\mu$ g) and Merg1b expression plasmid (30  $\mu$ g; 10). Seven days after electroporation (19), there was no significant difference in fiber csa of control muscle expressing lacZ alone ( $2456 \pm 13 \mu\text{m}^2$ , SEM) and those expressing lacZ and Merg1b ( $2449 \pm 16 \mu\text{m}^2$ , SEM). This finding suggests that the Merg1-induced significant decrease in fiber size is specific to the 1a variant.

### Astemizole dose-response curve

Three groups of three mice each were gavaged once every 12 h with a suspension of astemizole, a potent

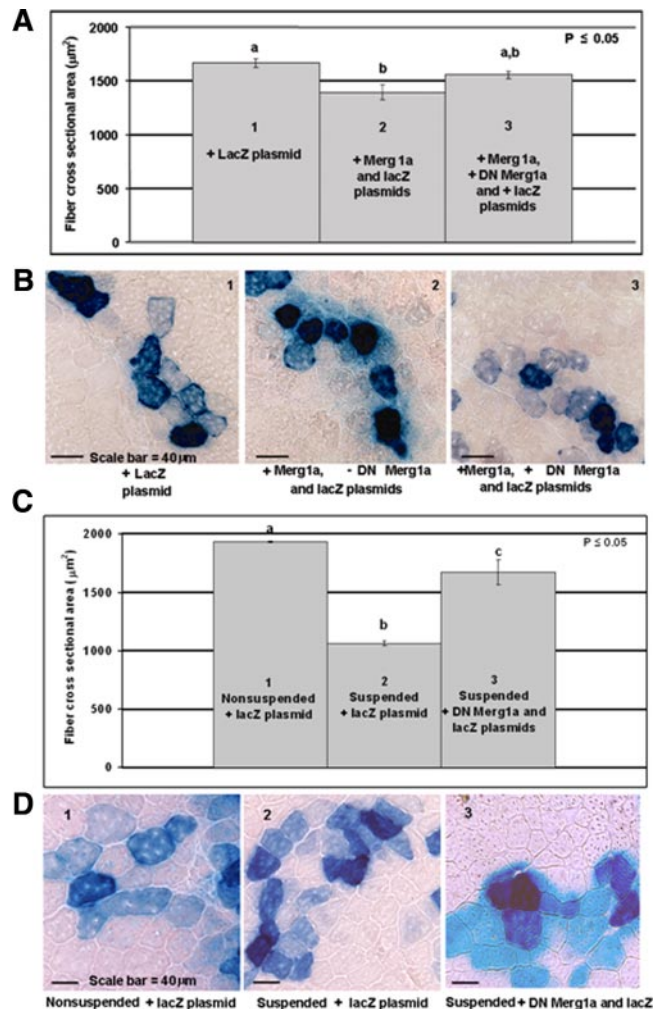


**Figure 3.** Block of Merg1a channel prevents onset of atrophy and ectopic expression of Merg1a induces skeletal muscle atrophy. Statistics. For both studies represented by this figure, changes in muscle fiber size were analyzed by ANOVA in a completely randomized design. In bar graphs, error bars indicate SE. Also, there are no statistical differences between groups with the same lower case letter and different letters indicate significant differences. *A*, *B*) Merg1a induces fiber size decrease while coexpression with the DN Merg1a mutant attenuates the decrease. Ectopic expression of Merg1a alone in wt-bearing mice ( $n=14$ ) results in a 16% decrease in fiber size (compare panels and bars 1 and 2). Although fibers expressing the dysfunctional DN Merg1a mutant in addition to Merg1a (panel and bar 3) did not remain at control size (panel and bar 1), they did retain 94% of control fiber cross-sectional area. *C*, *D*) Block of Merg1a channel function by expression of the DN Merg1a mutant prevents atrophy. Fibers from the gastrocnemius muscles of wt-bearing mice ( $n=7$ ) expressing lacZ (panel 1) were 45% larger than those in suspended mice ( $n=7$ ) expressing lacZ (panel and bar 2), demonstrating that hindlimb suspension induces skeletal muscle atrophy. LacZ expressing (blue) muscle fibers from the suspended mice receiving lacZ and DN Merg1a plasmids (panel and bar 3) were 36% larger than those of suspended mice not receiving DN Merg1a plasmid (panel 2).

erg1 channel blocker (20); to yield 80, 160, or 320 mg/kg body wt. A control group was gavaged with an equal vol. of water. ECGs and animal weights were measured daily. By treatment day seven, the corrected QT intervals (QTc's, 22) of all treated animals were significantly longer ( $P \leq 0.02$ ) than those of the control group, demonstrating that the drug blocked Merg1 channel in heart. Because wt loss was minimal and QTc prolongation was maximal, 160 mg/kg was used in the suspension study.

### Astemizole treatment inhibits atrophy in hindlimb-suspended mice and increases muscle size in wt-bearing controls

Twenty-eight mice were randomly assigned to four treatment groups. All animals received an oral gavage of water twice daily for 4 d. All mice were then gavaged once every 12 h for 7 d with either: water (groups 1 and 3) or 160 mg/kg astemizole in water (groups 2 and 4). During the 7 d, groups 1 and 2 remained wt-bearing, while groups 3 and 4 were subjected to hindlimb-suspension. Data (Table 1) show that astemizole treatment alone had no significant effect on body wt (note percent body wt change in groups 1 and 2). However, suspension caused a 7% decrease in body wt that was significantly alleviated by drug treatment (groups 3 and 4). Most importantly, the 15% decrease in muscle fiber csa that was experienced by hindlimb-suspended animals (groups 1 and 3) was blocked by astemizole treatment, bringing fiber csa values to control levels (compare groups 1 and 4). Interestingly, astemizole treatment produced significant increases in fiber csa, gastrocnemius muscle wt-to-body wt ratio and absolute gastrocnemius muscle wt in wt-bearing mice (groups 1 and 2). Data show that pharmacological block of Merg1 alleviates disuse atrophy and suggests that block of Merg1a function results in muscle hypertrophy. These effects likely result from decreased proteolysis produced by block of endogenous Merg1 channel. This is a reasonable supposition because we detect very low levels of Merg1a mRNA (Fig. 1C) and protein (Fig. 1D) in skeletal muscle of wt-bearing mice.

### Merg1a expression induces UPP activity

Mouse gastrocnemius muscles ( $n=26$ ) were injected with expression plasmids encoding Ub-FL (40  $\mu$ g; 18)

and the RL reporter (10  $\mu$ g). Activity of Ub-FL was normalized to RL activity to control for differences in the transfection efficiency from muscle to muscle. Ub-FL expression produces a measurable protein degraded by the UPP (18); the RL protein will not be degraded. Therefore, a reduction in the Ub-FL-to-RL activities ratio will represent an increase in UPP activity. Ub-FL and RL-injected mice ( $n=6$ ) also received a plasmid encoding Merg1a (30  $\mu$ g; 10), while others ( $n=7$ ) received the DN Merg1a mutant (30  $\mu$ g; 15). Remaining mice ( $n=13$ ) received control plasmids (30  $\mu$ g). Twelve hours after electroporation (19), mice injected with DN Merg1a ( $n=7$ ), and those injected with control plasmids ( $n=7$ ) were hindlimb-suspended, while other mice ( $n=12$ ) remained wt-bearing. After 7 d, ratios of Ub-FL-to-RL activity in gastrocnemius muscles were determined as measures of UPP activity; the lower ratios indicated higher UPP activity. Hindlimb suspension induced UPP activity (Fig. 4A1, 3). Ectopic expression of Merg1a in gastrocnemius muscles of wt-bearing mice induced proteolysis of Ub-FL, decreasing the Ub-FL-to-RL activity ratio by 48% relative to control (Fig. 4A3, 4). Also, block of endogenous Merg1a channel function by DN Merg1a expression significantly reduced UPP activity in suspended mice (Fig. 4A1, 2). Data show that Merg1a  $K^+$  channel function modulates UPP activity.

### Induction of UPP activity is Merg1a-specific

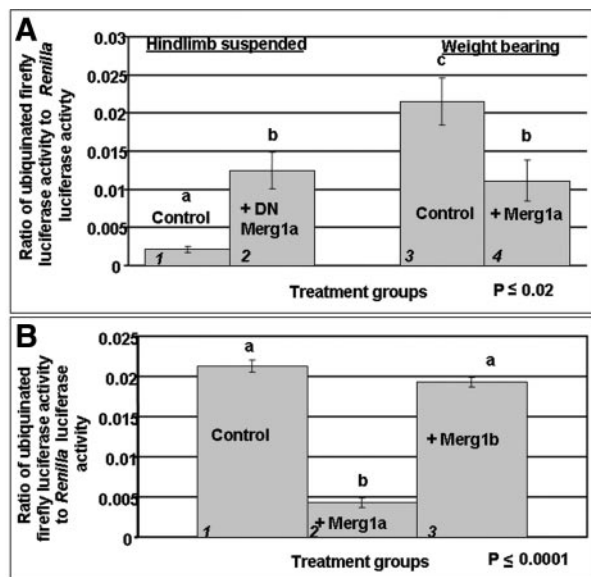
Both gastrocnemius muscles of 12 mice were coinjected with Ub-FL (40  $\mu$ g; 18) and RL (10  $\mu$ g) expression plasmids. The right gastrocnemius muscles of six of these mice were coinjected with Merg1a expression plasmid (30  $\mu$ g; 10), while right gastrocnemius muscles of the remaining six mice were coinjected with Merg1b expression plasmid (30  $\mu$ g; 10). Left gastrocnemius muscles received appropriate control plasmid (30  $\mu$ g). Seven days after electroporation (19), ectopic expression of Merg1a significantly increased UPP activity as evidenced by a decrease (80%) in the relative activity of Ub-FL (Fig. 4B1, 2); however, ectopic expression of Merg1b did not increase UPP activity as demonstrated by an insignificant (9.4%) decrease in the Ub-FL-to-RL ratio (Fig. 4A1, 3), an amount that could result from coassembly of Merg1b subunit with low levels of endog-

TABLE 1. Astemizole treatment (160 mg/kg) prevented skeletal muscle atrophy in hindlimb-suspended mice

	% Body weight change	Absolute gastrocnemius weight (g)	Gastrocnemius weight-to-body weight ratio	QTc interval	Fiber cross-sectional area ( $\mu\text{m}^2$ )
Group 1: Control	$7.0 \pm 0.12^a$	$0.19 \pm 0.006^a$	$0.58 \pm 0.033^a$	$28.2 \pm 0.5^a$	$1900 \pm 29.4^a$
Group 2: Astemizole	$5.9 \pm 0.6^a$	$0.21 \pm 0.005^b$	$0.66 \pm 0.015^b$	$27.9 \pm 0.4^a$	$2025 \pm 24.8^b$
Group 3: Suspension	$-7.0 \pm 1.5^c$	$0.17 \pm 0.160^c$	$0.59 \pm 0.018^{a,c}$	$26.0 \pm 0.9^b$	$1610 \pm 32.8^c$
Group 4: Astemizole & suspension	$-4.2 \pm 0.06^b$	$0.19 \pm 0.005^a$	$0.63 \pm 0.010^{b,c}$	$29.8 \pm 0.8^c$	$1841 \pm 29.4^a$

Data are reported as means  $\pm$  SE. Statements of significance are based on  $P \leq 0.05$ . There are no statistical differences between groups labeled with the same letter within a column. Different letters indicate significant differences within a column. QTc's are similar to those reported for mice anesthetized with Avertin (21).





**Figure 4.** Merg1a potassium channel regulates the ubiquitin-proteasome proteolytic pathway. Statistics. For both studies represented by this figure, changes in muscle Ub-FL-to-RL activity ratios were analyzed by ANOVA in a completely randomized design. Error bars indicate SE. There are no statistical differences between groups with the same lowercase letter. Different letters indicate significant differences. **A)** Ectopic expression of Merg1a enhances activity of the ubiquitin-proteasome pathway (UPP). Gastrocnemius muscles of mice were injected with plasmid DNA encoding ubiquitinated firefly luciferase (Ub-FL) and *Renilla* luciferase (RL) and electroporated. After 7 d, muscle homogenates were assayed for firefly and *Renilla* luciferase activities. The ratio of Ub-FL-to-RL activity indicates the concentration of UPP proteolysis; the lower ratios indicate higher UPP proteolytic activity levels. The ratio of Ub-FL-to-RL activity in the hindlimb-suspended mice not injected with DN-Merg1a (1) was significantly smaller (90%) than that measured in wt-bearing mice not injected with Merg1a (3). These data indicate that suspension induces UPP activity. Weight-bearing mice expressing Merg1a, RL, and Ub-FL (4) displayed a lower (48%) Ub-FL-to-RL activity ratio than wt-bearing mice expressing all these constructs except Merg1a (3). Data denote that Merg1a expression induces degradation of Ub-FL and, hence UPP activity. Suspended mice expressing the DN Merg1a nonfunctional mutant (2) display a significant 5.7-fold higher ratio of Ub-FL to RL activity than suspended mice not expressing DN Merg1a (1). These data show that block of the Merg1a channel can inhibit UPP mediated proteolysis. **B)** Increase in UPP activity is specific to the Merg1a alternative splice variant. Ratio of Ub-FL-to-RL activities in wt-bearing mice expressing Merg1a (2) was decreased by 80% relative to control animals (1). The ratio in mice expressing the Merg1b alternative splice variant (3), however, was decreased only by an insignificant 9.4% (3).

enous Merg1a. Data show that Merg1a, and not Merg1b, specifically increases UPP activity.

## DISCUSSION

Skeletal muscle health involves maintenance of an intricate balance between protein synthesis and degra-

dation. Atrophy results from a perturbation in this intricate modulation of the various synthetic and proteolytic pathways and very little is known about mechanisms involved in initiation of the imbalance (2, 3, 23). Our data demonstrate that Merg1a channel function participates in initiation of skeletal muscle atrophy in response to muscle disuse or cachexia by signaling an increase in UPP proteolysis. We show that Merg1 channel function is an initiating factor acting upstream of atrophy: 1) Merg1 proteins are detected [day 4 of suspension] before the onset of significant atrophy [day 7 of suspension]; 2) ectopic expression of Merg1a induces a decrease in fiber csa in wt-bearing limbs of mice; and 3) genetic and pharmacologic attenuation of Merg1 channel function prevents atrophy in hindlimb-suspended mice. Our studies also demonstrate that the Merg1a splice variant is expressed in skeletal muscle, while Merg1b is not detected, which strongly suggests that the Merg1 channel in this tissue is composed of Merg1a  $\alpha$  subunits only. Also, expression of Merg1a, and not Merg1b, results in decreased muscle fiber size and increased UPP activity in wt-bearing mice. Perhaps the more extensive Merg1a NH<sub>2</sub> terminus is necessary for up-regulation of the UPP. This portion of the protein does contain a number of unique signaling sequences, including a PAS-PAC domain, numerous potential protein kinase C (PKC) phosphorylation sites, a protein kinase A (PKA) phosphorylation site, and a potential cAMP/cGMP-dependent protein kinase phosphorylation site (10). Further, our data strongly suggest that Merg1a channel function is necessary to the atrophic process because both expression of the dysfunctional DN Merg1a mutant and astemizole treatment (pharmacologic channel block) inhibit the decrease in fiber size induced by suspension. Interestingly, although UPP activity is known to function during atrophic remodeling of the heart (24), physiologically relevant levels of Merg1 current ( $I_{Kr}$ ) are necessary for normal cardiac and are not likely to induce atrophy. Perhaps expression of the Merg1b splice variant in heart (12) is involved in this regulation. Therefore, the functional consequence of Merg1 channel current conduction may be determined by Merg1 channel  $\alpha$  subunit composition.

The possible mechanism(s) by which Merg1a function signals UPP activity is intriguing. It is known that HERG function is regulated by both PKC and PKA (25) and by PIP2 (26), serving as a link between adrenergic stimulation and regulation of the cardiac action potential. HERG channel function is also regulated by thyrotropin-releasing hormone (TRH) through G-proteins to mediate changes in the frequency of action potentials during the TRH response in GH<sub>3</sub> cells (27). Further, Merg1 function affects spike-frequency adaptation in neuroblastoma cells (28) and decreases the firing frequency of human  $\beta$ -cells (29). Interestingly, high-frequency stimulation of myoblasts from 20 d old rat embryos potentiates L-type Ca<sup>2+</sup> channels (by phosphorylation of the channel) and increases Ca<sup>2+</sup> flux through the sarcolemmal membrane (30). Perhaps,

Merg1 activity changes the response of skeletal myocytes to neural stimulation by modulating calcium channel activity. Merg1a activity may lower calcium flux across the sarcolemmal membrane and the concentration of depolarizing signal reaching the sarcoplasmic reticulum. Ultimately, the intracellular calcium concentration ( $[Ca^{2+}]_i$ ) would be decreased. Diminished  $[Ca^{2+}]_i$  precedes many of the functional changes resulting from hind-limb suspension (31), including the switch in predominant fiber type that occurs in slow twitch muscle undergoing atrophy; however, the mechanism(s) responsible for lowered  $[Ca^{2+}]_i$  is not well understood (31, 32). In summary, Merg1a channel function is an initiator of disuse- and cachexia-stimulated atrophy, acting upstream of UPP proteolysis. The mechanism involved in the modulation of UPP by Merg1a channel function obviously begs further study. **[F]**

The authors thank Dr. David Piwnica-Worms (Washington Univ.; St. Louis, MO) for his gift of plasmid encoding the ubiquitinated firefly luciferase. We thank Drs. Gordon Coppoc and Eli Asem (Purdue Univ.) for support. A.L.P. would like to thank Drs. Jeanne M. Nerbonne (Washington University School of Medicine; St. Louis, MO) and David Van Wagoner (Cleveland Clinic Foundation; Cleveland, OH) for helpful discussions about ion channel physiology. This project was funded in large part by the American Heart Association (Scientist Development Grant #0235363N to ALP) and in part by USDA-CSREES Hatch Project number INDO76045 and the Purdue University Department of Basic Medical Sciences.

## REFERENCES

- McArdle, A., Dillmann, W. H., Mestrlil, R., Faulkner, J. A., and Jackson, M. J. (2004) Overexpression of HSP70 in mouse skeletal muscle protects against muscle damage and age-related muscle dysfunction. *FASEB J.* **18**, 355–357
- Haddad, F., Roy, R. R., Zhong, H., Edgerton, V. R., and Baldwin, K. M. (2003) Atrophy responses to muscle inactivity. II. Molecular markers of protein deficits. *J. Appl. Physiol.* **95**, 791–802
- Glass, D. J. (2003) Signalling pathways that mediate skeletal muscle hypertrophy and atrophy. *Nat. Cell Biol.* **5**, 87–90
- Franch, H. A., and Price, S. R. (2005) Molecular signaling pathways regulating muscle proteolysis during atrophy. *Curr. Opin. Clin. Nutr. Metabol. Care* **8**, 271–275
- Rommel, C., Bodine, S. C., Clarke, B. A., Rossman, R., Nunez, L., Stitt, T. N., Yancopoulos, G. D., and Glass, D. J. (2001) Mediation of IGF-1-induced skeletal myotube hypertrophy by PI(3)K/Akt/mTOR and PI(3)K/Akt/GSK3 pathways. *Nat. Cell Biol.* **3**, 1009–1013
- Tawa, N.E. Jr., Odessey, R., and Goldberg, A. L. (1997) Inhibitors of the proteasome reduce the accelerated proteolysis in atrophying rat skeletal muscles. *J. Clin. Invest.* **100**, 197–203
- Semsarian, C., Wu, M. J., Ju, Y. K., Marciniak, T., Yeoh, T., Allen, D. G., Harvey, R. P., and Graham, R. M. (1999) Skeletal muscle hypertrophy is mediated by a  $Ca^{2+}$ -dependent calcineurin signaling pathway. *Nature* **400**, 576–581
- Bodine, S. C., Latres, E., Baumhueter, S., Lai, V. K., Nunez, L., Clarke, B. A., Poueymirou, W. T., Panaro, F. J., Na, E., Dharmarajan, et al. (2001) Identification of ubiquitin ligases required for skeletal muscle atrophy. *Science* **294**, 1704–1708
- Curran, M. E., Splawski, I., Timothy, K. W., Vincent, G. M., Green, E. D., and Keating, M. T. (1995) A molecular basis for cardiac arrhythmia: *herg* mutations cause long QT syndrome. *Cell* **80**, 795–803
- London, B., Trudeau, M. C., Newton, K. P., Beyer, A. K., Copeland, N. G., Gilbert, D. J., Jenkins, N. A., Satler, C. A., and Robertson, G. A. (1997) Two isoforms of the mouse ether-a-go-go-related gene coassemble to form channels with properties similar to the rapidly activating component of the cardiac delayed rectifier  $K^+$  current. *Circ. Res.* **81**, 870–878
- Lees-Miller, J.P., Kondo, C., Wang, L., and Duff, H. J. (1997) Electrophysiological characterization of an alternatively processed ERG  $K^+$  channel in mouse and human hearts. *Circ. Res.* **81**, 719–726
- Jones, E. M., Roti, E. C., Wang, J., Delfosse, S. A., and Robertson, G. A. (2004) Cardiac  $I_{Kr}$  channels minimally comprise hERG 1a and 1b subunits. *J. Biol. Chem.* **279**, 44690–44694
- Polvani, S., Masi, A., Pillozzi, S., Gragnani, L., Crociani, O., Olivotto, M., Becchetti, A., Wanke, E., and Arcangeli, A. (2003) Developmentally regulated expression of the mouse homologues of the potassium channel encoding genes m-erg1, m-erg2 and m-erg3. *Gene Expr. Patterns* **3**, 767–776
- Pond, A. L., Scheve, B. K., Benedict, A. T., Petrecca, K., Van Wagoner, D. R., Shrier, A., and Nerbonne, J. M. (2000) Expression of distinct ERG proteins in rat, mouse and human heart. *J. Biol. Chem.* **275**, 5997–6006
- Selyanko, A. A., Delmas, P., Hadley, J. K., Tatulian, L., Wood, I. C., Mistry, M., London, B., and Brown, D. A. (2002) Dominant-negative subunits reveal potassium channel families that contribute to M-like potassium currents. *J. Neurosci.* **22**, RC212–217
- Alzghoul, M.B., Gerrard, D., Watkins, B. A., and Hannon, K. (2004) Ectopic expression of IGF-1 and Shh by skeletal muscle inhibits disuse-mediated skeletal muscle atrophy and bone osteopenia in vivo. *FASEB J.* **18**, 221–223
- Matsushita, S., Nitanda, T., Furukawa, T., Sumizawa, T., Tani, A., Nishimoto, K., Akiba, S., Miyadera, K., Fukushima, M., Yamada, Y., et al. (1999) The effect of a thymidine phosphorylase inhibitor on angiogenesis and apoptosis in tumors. *Cancer Res.* **59**, 1911–1916
- Luker, G. D., Pica, C. M., Song, J., Luker, K. E., and Piwnica-Worms, D. (2003) Imaging 26S proteasome activity and inhibition in living mice. *Nat. Med.* **9**, 969–973
- Taylor, J., Babbs, C.F., Alzghoul, M.B., Olsen, A., Latour, M., Pond, A. L., and Hannon, K. (2004) Optimization of ectopic gene expression in skeletal muscle through DNA transfer by electroporation. *BMC Biotechnol.* **4**, 11
- Zhou, Z., Vorperian, V. R., Gong, Q., Zhang, S., and January, C. T. (1999) Block of HERG potassium channels by the antihistamine astemizole and its metabolites desmethyastemizole and norastemizole. *J. Cardiovasc. Electrophysiol.* **10**, 836–843
- Kirchhoff, S., Nelles, E., Hagedorff, A., Kruger, O., Traub, O., and Willecke, K. (1998) Reduced cardiac conduction velocity and predisposition to arrhythmias in connexin40-deficient mice. *Curr. Biol.* **8**, 299–302
- Mitchell, G.F., Jeron, A., and Koren, G. (1998) Measurement of heart rate and Q-T interval in the conscious mouse. *Am. J. Physiol.* **274**, H747–H751
- Jackman, R., and Kandarian, S. C. (2004) The molecular basis of skeletal muscle atrophy. *Am. J. Physiol. Cell Physiol.* **287**, 834–843
- Razeghi, P., Sharma, S., Ying, J., Li, Y. P., Stepkowski, S., Reid, M. B., and Taegtmeier, H. (2003) Atrophic remodeling of the heart in vivo simultaneously activates pathways of protein synthesis and degradation. *Circ.* **108**, 2536–2541
- Thomas, D., Kiehn, J., Katus, H. A., and Karle, C. A. (2004) Adrenergic regulation of the rapid component of the cardiac delayed rectifier potassium current,  $I(Kr)$ , and the underlying hERG ion channel. *Basic Res. Cardiol.* **99**, 279–287
- Bian, J.-S., Kagan, A., and McDonald, T. V. (2004) Molecular analysis of PIP2 regulation of HERG and  $I(Kr)$ . *AJP-Heart* **287**, 2154–2163
- Miranda, P., Giraldez, T., de la Pena, P., Manso, D. G., and Alonso-Ron, C. (2005) Specificity of TRH receptor coupling to G-proteins for regulation of ERG  $K^+$  channels in GH<sub>3</sub> rat anterior pituitary cells. *J. Physiol.* **566**, 717–736
- Chiesa, N., Rosati, B., Arcangeli, A., Olivotto, M., and Wanke, E. (1997) A novel role for HERG  $K^+$  channels: spike-frequency adaptation. *J. Physiol.* **501**, 313–318
- Rosati, B., Marchetti, P., Crociani, O., Lecchi, M., Lupi, R., Arcangeli, A., Olivotto, M., and Wanke, E. (2000) Glucose- and arginine-



- induced insulin secretion by human pancreatic  $\beta$ -cells: the role of HERG  $K^+$  channels in firing and release. *FASEB J.* **14**, 2601–2610
30. Sculptoreanu, A., Scheuer, T., and Catterall, W. A. (1993) Voltage-dependent potentiation of L-type  $Ca^{2+}$  channels due to phosphorylation by cAMP-dependent protein kinase. *Nature* **364**, 240–243
  31. Fraysse, B., Desaphy, J. F., Pierno, S., De Luca, A., Liantonio, A., Mitolo, C. I., and Camerino, D. C. (2003) Decrease in resting calcium and calcium entry associated with slow-to-fast transition in unloaded rat soleus muscle. *FASEB J.* **17**, 1916–1918
  32. Pette, D., and Staron, R. S. (2001) Transitions of muscle fiber phenotypic profiles. *Histochem. Cell Biol.* **115**, 359–372

*Received for publication November 18, 2005.*  
*Accepted for publication February 16, 2006.*

# Merg1a K<sup>+</sup> channel induces skeletal muscle atrophy by activating the ubiquitin proteasome pathway

Xun Wang,\* Gregory H. Hockerman,<sup>†</sup> Henry W. Green III,<sup>‡</sup> Charles F. Babbs,\* Sulma I. Mohammad,<sup>§</sup> David Gerrard,<sup>¶</sup> Mickey A. Latour,<sup>¶</sup> Barry London,<sup>¶</sup> Kevin M. Hannon,\*<sup>1</sup> and Amber L. Pond\*<sup>1,2</sup>

\*Department of Basic Medical Sciences, School of Veterinary Medicine; <sup>†</sup>Department of Medicinal Chemistry and Molecular Pharmacology, College of Pharmacy; <sup>‡</sup>Department of Veterinary Clinical Sciences, School of Veterinary Medicine; <sup>§</sup>Department of Veterinary Pathobiology and Cancer Center; and <sup>¶</sup>Department of Animal Sciences, College of Agriculture, Purdue University, West Lafayette, Indiana, USA; and <sup>1</sup>Cardiovascular Institute, University of Pittsburgh, Pittsburgh, Pennsylvania, USA



To read the full text of this article, go to <http://www.fasebj.org/cgi/doi/10.1096/fj.05-5350fje>

## SPECIFIC AIMS

The goals of this study were to: 1) demonstrate that Merg1a K<sup>+</sup> channel is expressed endogenously in skeletal muscle (skm) undergoing atrophy as a result of disuse and malignant tumor expression; 2) determine if ectopic expression of Merg1a induces skm atrophy in wt-bearing mice and if this effect can be inhibited by coexpression of Merg1a and the nonfunctional dominant-negative DN-Merg1a; 3) determine if inhibition of Merg1 channel function by ectopic expression of DN-Merg1a inhibits onset of atrophy in hindlimb-suspended mice; 4) administer the Merg1a blocker astemizole to hindlimb-suspended and wt-bearing mice to determine if pharmacological block of this channel will block atrophy in skm; and 5) determine if ectopic expression of Merg1a will specifically increase the concentration of ubiquitin proteasome proteolysis, the pathway responsible for the majority of protein degradation that occurs during skm atrophy.

## PRINCIPAL FINDINGS

### 1. Tumor expression and hindlimb suspension result in skeletal muscle atrophy and Merg1a synthesis

Kb human esophageal cancer were implanted subcutaneously (s.c.) in the right axilla of athymic mice NCr-nu; Harlan, IN) while control mice were injected with vehicle. ND4-Swiss Webster mice were placed in suspension cages so that they were unable to place any load on their hindlimbs. Control mice were kept in a normal wt-bearing state. After six weeks, the mean muscle fiber cross-sectional area (csa) of gastrocnemius muscles from tumor-bearing mice was 25% less ( $P \leq 0.05$ , ANOVA) than that of control mice. After 7 d, hindlimb-suspended mice experienced a 45% decrease ( $P \leq 0.05$ ) in muscle fiber csa relative to wt-bearing controls,

denoting significant atrophy. Western blot analysis of extracted membrane proteins detected Merg1a proteins in both cachectic and suspended mouse skm (Fig. 1A, B), but not in control tissue unless it was concentrated 4-fold (Fig. 1C). Merg1a mRNA was readily detected in gastrocnemius muscles of suspended mice, while only low levels were detected in control skm. Neither Merg1b protein nor mRNA was detected in suspended or control mouse skm (Fig. 1A). Immunostained sections from suspended mice revealed that Merg1 protein is located in sarcolemmal membranes of myocytes, while it is undetected in control skm (Fig. 1D).

### 2. Ectopic expression of Merg1a induces skeletal muscle atrophy in wt-bearing mice, while coexpression of Merg1a and the dominant-negative DN-Merg1a attenuates the decrease in myofiber size

Injection of plasmid DNA into skm followed by electroporation resulted in expression of encoded genes, specifically Merg1a and Merg1b, as verified with Western blot analysis. We injected the left gastrocnemius muscles of 14 mice with lacZ and control expression plasmids. Right gastrocnemius muscles of seven of these mice were coinjected with Merg1a, lacZ, and control expression plasmids. The right gastrocnemius muscles of the remaining mice were coinjected with three expression plasmids, each encoding either: Merg1a, lacZ, or a DN Merg1a mutant. (The DN Merg1a gene product is a pore mutant that is transported to the cell membrane but prevents Merg1 current conduction.) Mice remained wt bearing. Seven

<sup>1</sup> These authors contributed equally to this work.

<sup>2</sup> Correspondence: School of Veterinary Medicine, Purdue University, 625 Harrison St., West Lafayette, IN 47907, USA. E-mail: [pond@purdue.edu](mailto:pond@purdue.edu)  
doi: 10.1096/fj.05-5350fje

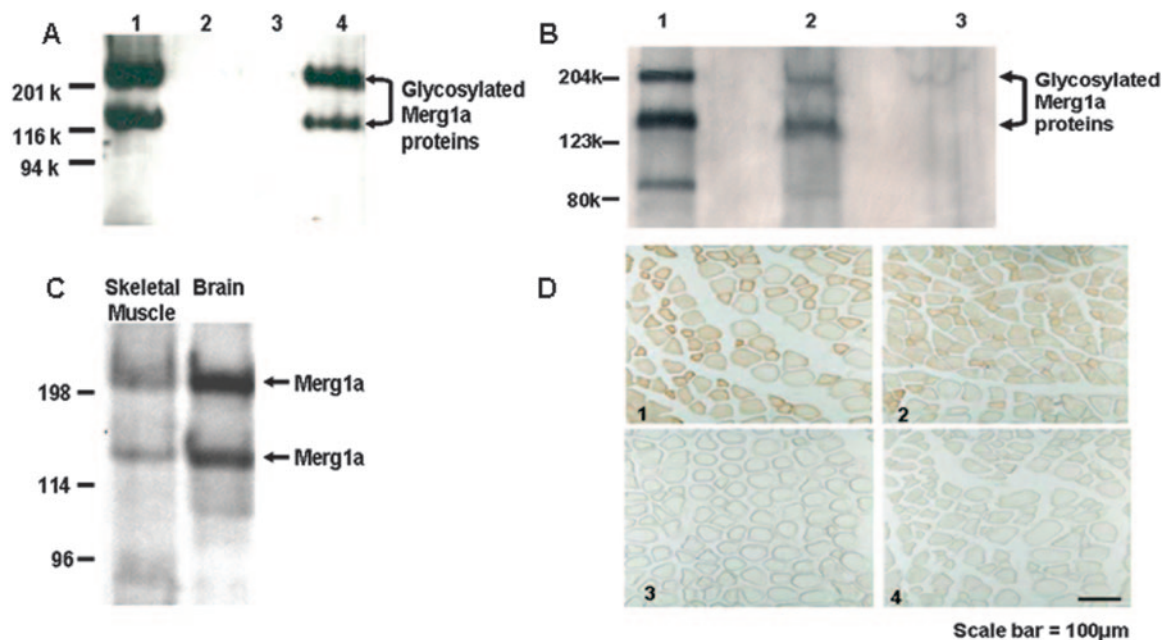


**Figure 1.** Merg1a  $K^+$  channel is expressed in atrophic gastrocnemius muscles of cachectic and hindlimb-suspended mice. *A*) Merg1a channel protein isoforms are detected in gastrocnemius muscles of mice experiencing atrophy as a result of malignant tumor growth. Western blot of membrane protein fractions from brain (lane 1 positive control, 15  $\mu$ g), control mouse gastrocnemius muscle (pooled muscles of 8 mice; lanes 2 and 3, 50 and 44  $\mu$ g, respectively) and tumor-expressing mouse gastrocnemius muscle (pooled muscles of 8 mice; lane 4, 44  $\mu$ g). *B*) Merg1a proteins are detected in gastrocnemius muscles of hindlimb-suspended mice. Western blot of membrane proteins from brain (lane 1 positive control, 15  $\mu$ g), skm from suspended mice (pooled muscles of 10 mice; lane 2, 60  $\mu$ g), and skm from wt-bearing mice (pooled muscles of 10 mice; lane 3, 60  $\mu$ g). *C*) Low levels of Merg1a protein are detected in skm of wt-bearing mice. Western blot of membrane protein fractions from control mouse gastrocnemius muscle concentrated fourfold (lane 1, 70  $\mu$ g) and from brain sample (lane 2, 15  $\mu$ g). *D*) Merg1a  $K^+$  channel protein is located in sarcolemmal membranes of skeletal muscle from hindlimb-suspended mice. Representative muscle sections from animals suspended for 4 (panel 1) and 7 (panel 2) d and immunostained with erg1 Ab. Representative muscle section (immunostained with erg1 Ab) from a wt-bearing animal (panel 3). Representative muscle section from suspended (4 d) mouse immunostained without erg1 Ab (panel 4) as control.

days after electroporation, gastrocnemius fibers expressing Merg1a and lacZ experienced a significant ( $P \leq 0.05$ , ANOVA) 16.3% decrease in muscle fiber cross-sectional area (csa) relative to fibers injected with lacZ plasmid only. Blockade of Merg1a function by DN Merg1a prevented all but 6.7% of the atrophy induced by Merg1a expression. This incomplete rescue is expected because it is not likely that all randomly assembled channels would contain mutant channel subunit.

### 3. Inhibition of Merg1 channel function by ectopic expression of DN-Merg1a inhibits the onset of atrophy in hindlimb-suspended mice

We injected left gastrocnemius muscles of 14 mice with lacZ and control expression plasmids. Right gastrocnemius muscles received lacZ plasmid plus expression plasmid encoding DN Merg1a. Mice were then either hindlimb-suspended ( $n=7$ ) or remained wt bearing ( $n=7$ ). After 7 d, there was a 45% decrease ( $P \leq 0.05$ , ANOVA) in csa of suspended mouse myofibers expressing lacZ relative to wt-bearing controls expressing lacZ, showing that suspension induced atrophy. Importantly, muscle fibers from suspended mice expressing lacZ and DN Merg1a mutants were 13.4% smaller than control

muscle fibers. Block of Merg1a function does attenuate atrophy. Thus, synthesis of DN Merg1a mutant blocks the onset of disuse atrophy in suspended mice, showing that Merg1a current conduction plays a role in atrophy induction. Further, there was no significant difference in fiber csa of control muscle expressing lacZ alone and those expressing lacZ and Merg1b. This finding suggests that Merg1-induced significant decrease in fiber size is specific to the Merg1a variant.

### 4. Pharmacological block of the Merg1 channel with astemizole inhibits atrophy in hindlimb-suspended mice and promotes myofiber growth in skeletal muscle of wt-bearing mice

Twenty-eight mice were orally gavaged once every 12 h for 7 d with either: water (groups 1 and 3) or 160 mg/kg astemizole in water (groups 2 and 4). During treatment, groups 1 and 2 remained wt-bearing, while groups 3 and 4 were hindlimb-suspended. Data show that astemizole treatment alone had no significant effect on body wt of wt-bearing mice; however, suspension caused a significant ( $P \leq 0.05$ , ANOVA) 7% decrease in body wt that was significantly alleviated by drug treatment. Most importantly, the 15% decrease in muscle fiber csa that was experienced by hindlimb-



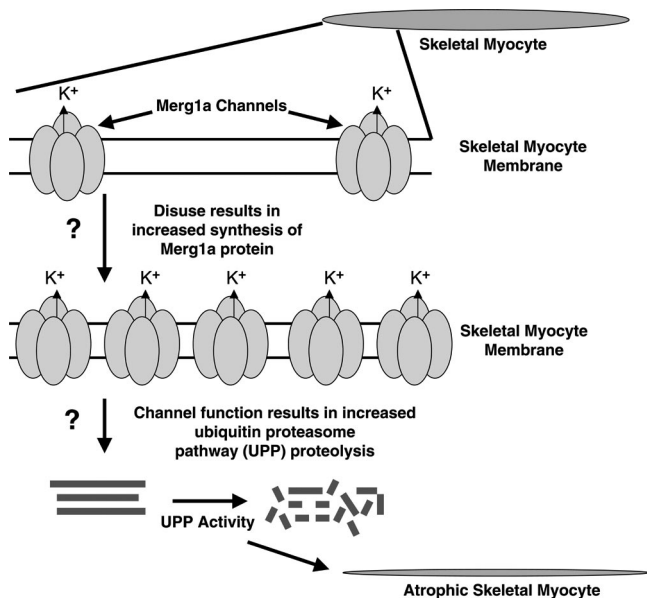


**Figure 2.** Schematic representation demonstrating that the Merg1a channel is up-regulated in response to skm disuse and that channel function yields an increase in the ubiquitin proteasome proteolysis that participates in the atrophic process. Two obvious areas of needed research are highlighted by questions marks: 1) by what process does disuse signal the up-regulation of Merg1a protein; and 2) by what mechanism does Merg1a function signal UPP activity.

suspended animals was blocked by astemizole treatment, bringing fiber csa values to control levels. Interestingly, astemizole treatment produced significant increases in fiber csa, gastrocnemius muscle wt to body wt ratio, and absolute gastrocnemius muscle wt in control mice. Data show that pharmacological block of Merg1 alleviates disuse atrophy and suggests that block of Merg1a function results in muscle hypertrophy.

### 5. Ectopic expression of Merg1a increases the concentration of ubiquitin proteasome proteolysis

Expression of ubiquitinated firefly luciferase reporter (Ub-FL) produces a measurable protein degraded by the ubiquitin proteasome pathway (UPP). We injected gastrocnemius muscles with two expression plasmids, one encoding Ub-FL and the other *Renilla* luciferase (*RL*). Muscles were electroporated. Ub-FL- and *RL*-injected mice also received plasmid encoding: either Merg1a or DN Merg1a or control plasmid. Mice injected with DN Merg1a or control plasmid were hindlimb-suspended, while the remaining control mice and those injected with Merg1a remained wt-bearing. Ub-FL activity was normalized to *RL* activity to control for differences in muscle transfection efficiency, and ratios of Ub-FL to *RL* activity were determined as measures of UPP activity; lower ratios indicated higher UPP activity. The Ub-FL-to-*RL* activity ratio in hindlimb-suspended mice not injected with DN-Merg1a was 90% smaller ( $P \leq 0.02$ ; ANOVA) than that measured in wt-bearing mice not injected with Merg1a. Data indi-

cate that suspension induces UPP activity. Weight-bearing mice expressing Merg1a, *RL*, and Ub-FL displayed a 48% lower ( $P \leq 0.02$ ) Ub-FL to *RL* activity ratio than wt-bearing mice expressing all constructs except Merg1a, denoting that Merg1a expression induces UPP activity. Suspended mice expressing DN Merg1a displayed a 5.7-fold higher ( $P \leq 0.02$ ) Ub-FL to *RL* activity ratio than suspended mice not expressing DN Merg1a, showing that block of Merg1 channel inhibits UPP proteolysis. The Ub-FL-to-*RL* ratio in gastrocnemius muscles coexpressing Merg1b (rather than Merg1a) show that ectopic expression of Merg1b decreased UPP activity by an insignificant 9.4%, an amount that may result from coassembly of Merg1b subunit with low levels of endogenous Merg1a. Thus, Merg1a specifically increases UPP activity.

## CONCLUSIONS AND SIGNIFICANCE

We know of no other reports linking Merg1 (or the human homologue HERG)  $K^+$ -channel function to skeletal muscle atrophy. We show that Merg1 channel function is, in fact, an initiating factor of skm atrophy: 1) Merg1 proteins are detected before onset of significant atrophy; 2) ectopic expression of Merg1a induces a decrease in fiber csa in skm of wt-bearing mice; and 3) genetic and pharmacologic block of Merg1 channel function strongly attenuates atrophy in hindlimb-suspended mice. Additionally, data suggest that block of endogenous Merg1 in normal mice induces hypertrophy. Data also strongly imply that Merg1a channel function participates in initiation of skeletal muscle atrophy by signaling an increase in UPP activity, a pathway known to be responsible for a large portion of the protein degradation that occurs during skm atrophy. Despite recent advances, little is known about initiation of UPP activity and factors acting upstream of the atrophic process. We have discovered that a membrane protein, one capable of sensing and responding to changes in membrane potential, is up-regulated prior to onset of significant atrophy and, in fact, induces an increase in activity of the UPP pathway. We find no other reports linking Merg1 function to UPP activity.

Obviously, the mechanism by which Merg1a channel function induces UPP activity begs elucidation. This information is of interest to skm researchers because the Merg1a channel gene and protein are now potential targets for therapies designed to treat skm atrophy. It is, in fact, relevant to researchers in any field involving UPP proteolysis and particularly the cardiac field. For example, UPP activity participates in atrophic remodeling of the heart; however, physiologically relevant levels of Merg1 current ( $I_{Kr}$ ) are necessary for normal cardiac function. Perhaps expression of the Merg1b splice variant or another  $K^+$  channel subunit in heart is involved in this regulation. Therefore, the functional consequence of Merg1 channel expression may be determined by Merg1 channel subunit composition.

**FJ**